Structural Eng. / Earthquake Eng. Vol. 7. No. 2, 293s-304s. October 1990
Japan Society of Civil Engineers (Proc. of JSCE No. 422/I-14)

FIELD TESTS AND ANALYSIS OF A GLUED-LAMINATED TIMBER BEAM BRIDGE

By Seizo USUKI and Richard M. GUTKOWSKI***

The Uyashinai bridge is located on the Uyashinai forest road in Akita Regional Forest Office. This bridge is a glued-laminated grillage girder bridge with timber deck panels and steel diaphragms. The present paper is concerned with the development of an analytical model and studying the field behavior of the bridge. A method of incorporating the rigidity of the diaphragms in the analysis is presented. Full-scale tests of the Uyashinai forest road bridge are studied experimentally and are compared with the numerical solutions. Through the comparison with field test results, the accuracy and the efficiency of the proposed method is verified.

Keywords: *bridge, diaphragms, field test, grillage stiffness, glued-laminated*

1. INTRODUCTION

In early times, logging bridges were commonly used in Japan. In 1940, the Specification for Timber Bridge Design[1] was enacted by the Ministry of Construction. The most common deck system used was a nail-laminated assembly of thick lumber placed transverse to the supporting stringers. The deck timber was pressure-treated with creosote and the sandy soil served as a wearing surface[2]. The bridges were designed to carry trucks weighing 9 tons.

After the World War II, however, because forest products were already exhausted and because the reconstruction of impoverished land required heavily-loaded transporting trucks, the logging bridges have been abandoned entirely (since the middle 1950's). The primary materials of bridge construction are currently limited to concrete, normal steel and special steel alloys.

On the other hand, in foreign countries, particularly in the U. S. A. and Canada, various types of modern timber bridges have been developed. The glued-laminated (glulam) stringer has taken the place of the native round log stringer and the glulam deck panel has replaced the nail-laminated deck. Glulam is an assembly of individual wood laminae bonded together with structural adhesive. The net thickness of any individual lamination does not exceed 5 cm (2 in.). Research to establish allowable design stresses related to the various laminating combinations dates back to the early 1940's. Exellent summaries of the investigation of glulam stress design are given by Gutkowski and Williamson[3),4)]. Structural research needs pertinent to heavy timber are also presented by these authors[5)].

On the basis of the results of this recent research in the U. S., the bridge specifications of the American Association of State Highway and Transportation Officials (AASHTO)[6] provide criteria for glulam

* Member of JSCE, Dr. Eng., Professor, Department of Civil Engineering, Akita University (Tegatagakuen, Akita, 010, Japan)
** Ph. D., Professor, Department of Civil Engineering, Colorado State University (Fort Collins, Colorado, 80523, U. S. A.)

allowable stresses, glulam bridge design, load distribution factors, and so on. Similar efforts have also been undertaken in Canada and Scarisbrick[7] has reported developments of glulam timber bridges in British Columbia.

The cross-section of a glulam timber beam can be manufactured in various types of large shapes, such as I-beams and rectangular beams, without utilizing expensive, large, high quality logs. By the introduction of preservative treatments such as creosote, the meterial life of timber bridges can be extended to 50 years or more[8].

The present paper is concerned with the Uyashinai Bridge which was constructed in the suburbs of Akita-City, Japan as a forest roadway bridge. The construction was completed in August, 1988. The design procedure of the bridge is based on the Specifications and Commentaries for Roadway Bridges of Japan[9] with respect to loadings and on the Specifications and Commentaries for Timber Construction of JSAE[10] with respect to allowable design stresses.

Field tests under static truck loadings were conducted and the test results are compared with numerical solutions based on the grillage bridge analysis. Studies of glulam bridge decks with or without dowel connections have been presented by McCutcheon and Tuomi[11,12], Tuomi and McCutcheon[13], Tuomi[14], and Gutkowski[15]. Sanders has studied the load distribution in glulam bridges[16]. These studies were, however, either concerned with deck systems or reduced-size bridge models. The reports on field tests of actual glulam timber bridges and on their theoretical verifications can rarely been found.

2. A STATIC MODEL OF DIAPHRAGM AND CROSS BOLTS

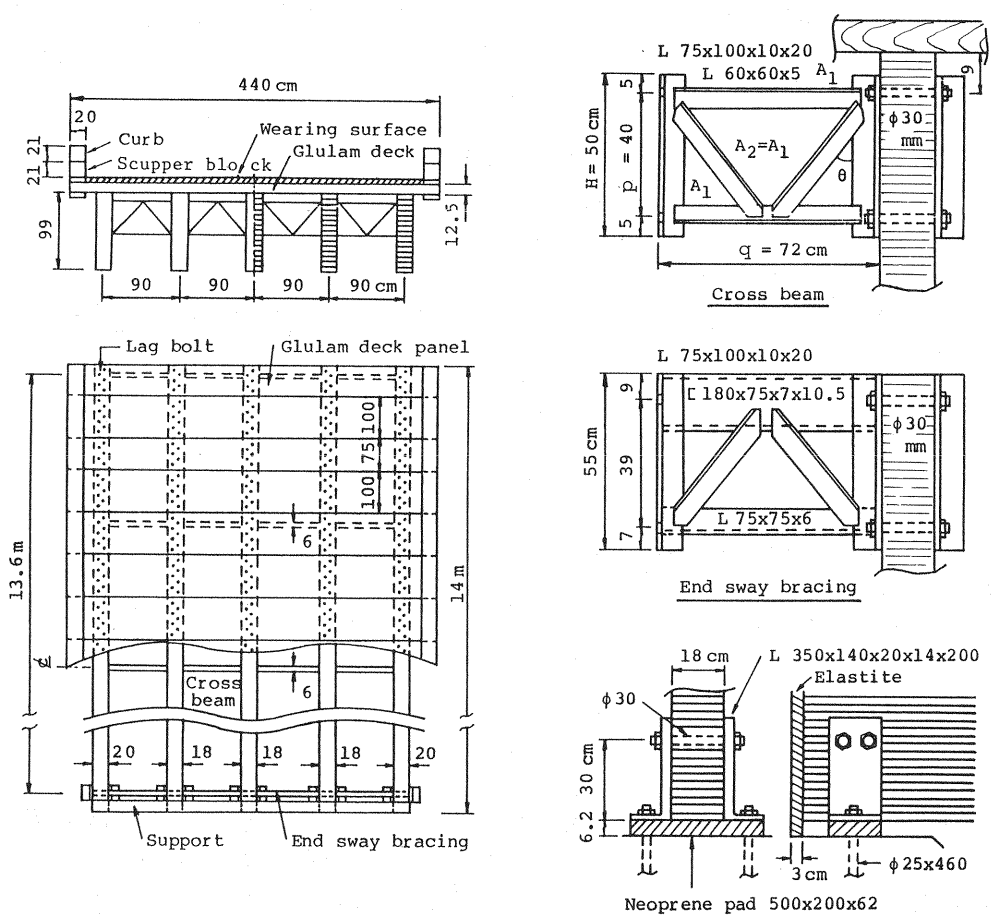

Fig. 1 General views of the diaphragms and the shoe of the Uyashinai Bridge.

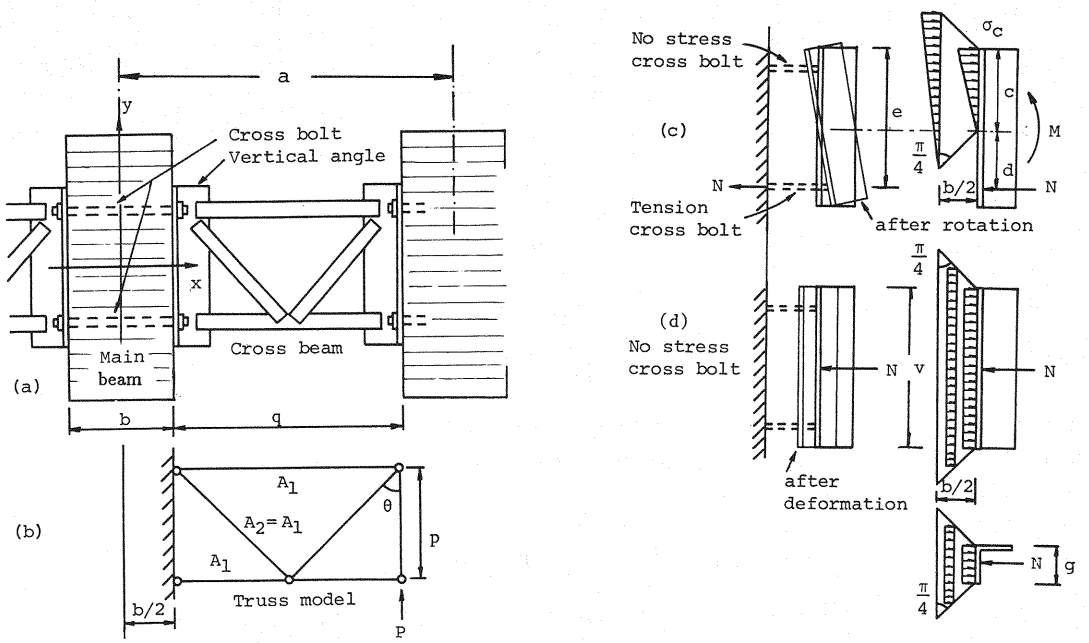

Fig. 2 (a) diaphragm, (b) truss model of cross beam, (c) stress distribution due to bending, (d) stress distribution due to axial force.

Fig. 1 shows the general views, diaphragm, end sway bracing, and bearing pad of the Uyashinai Bridge. The asphalt pavement used as a wearing surface has an average thickness of 7 cm and the thickness of laminae of all glulam timbers is 3 cm. The T-14 loadings are used as live loads. The cross-sectional dimensions of the diaphragms and cross bolts as well as the main beams are designed for shear and bending moment due to live loads, dead loads and snow loads, based on the assumption of the grillage stiffness model. The transverse framing system of the bridge consists of steel truss type diaphragms bolted through the beams. The bolts fasten adjacent diaphragms only by tightening the nuts. A procedure for estimating bending rigidities of diaphragms is presented in Ref. 17), 18) by Usuki, *et al.* Here, for convenience to the present study, the basic formulas presented in Ref. 17), 18) are briefly summarized.

(1) Bending rigidity of diaphragm and cross bolts

In Fig. 2(a), the L-shaped members of a diaphragm are shown. Then, as shown in Fig. 2(b), the diaphragm is replaced by a simple truss model for estimating bending rigidity. The symbols A_1 and A_2 represent the cross-sectional areas of the members. The moment of inertia of the truss model is based on equivalence to a corresponding cantilever beam (see Ref. 19)). On the other hand, the widths of the main timber beams are large compared to the thickness of the deck. In the case of the Uyashinai forest roadway bridge, the ratio of the beam width to on-center spacing of the beams, that is, b/a, is equal to either 20 cm/90 cm or 18 cm/90 cm, i. e. non-dimensional ratios of either 1/4.5 or 1/5.0, respectively, (see Fig. 1). Thus, we must consider the diaphragms shown in Fig. 2(a) as a cross beam having a short span.

We assume that when a bending moment M acts at a diaphragm, the L-shaped vertical member of the diaphragm connected to the side of the main timber beam rotates as a rigid body, as shown in Fig. 2(c). When the applied bending moment is positive, the upper cross bolt has no stress and the lower cross bolt has tensile stress. On the side of the main beam, a reactive normal stress occurs over a bearing area $c \times g$. We can reasonably assume that the magnitude of the reactive normal stress is proportional to that of the horizontal displacement of the vertical angle member and that the reactive normal stress on the bearing surface is distributed into the timber main beam prismatically, as shown in Fig. 2(c).

From the above assumptions, we can obtain the location of the neutral axis having the distance d from

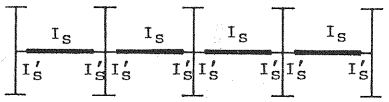

Fig. 3 Idealized model of the diaphragm.

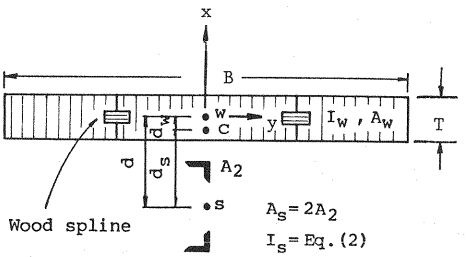

Fig. 4 Cross section of the composite cross beam.

lower cross bolt, the reactive stress σ_c at the upper tip of vertical angle and the normal force acting at the lower cross bolt. With these values known, we can estimate the strain energy stored within the timber beam and cross bolt in terms of the acting bending moment M as being equal to that of the steel truss diaphragm. Thus, the corresponding moment of inertia becomes :

$$I'_s=\frac{3A_m\frac{1}{n'}b(c-g)\left(d+\frac{2}{3}c\right)^2}{4A_m\cdot\ln\frac{c(g+b)}{g(c+b)}+\frac{3}{n'}(c-g)b}, \quad \cdots\cdots (1)$$

where $n'=E_s/E_{\perp x}$, and $E_{\perp x}$=Young's modulus of the glulam timber in the x-direction (perpendicular to grain), as shown in Fig. 2(a). E_s and A_m are Young's modulus and sectional area of the cross bolt, respectively. The moment of inertia of the diaphragms is conventionally given as[19]

$$I_s=\frac{A_1p^2/2}{1.0+\frac{3A_1p^2/2}{A_2q^2\sin\theta}}. \quad \cdots\cdots (2)$$

The proposed static model of the diaphragm system is illustrated in Fig. 3.

(2) Bending rigidity of composite diaphragm and cross bolts

As can be seen in Fig. 1 the glulam deck panels are attached to the main beams using threaded lag bolts. The deck panels are continuous in the transverse direction of the bridge axis, but discontinuous in the longitudinal direction of the bridge axis. Thus, we can expect composite action of the deck panels and diaphragms with respect to the bending of diaphragm systems about the bridge axis. Gutkowski, *et al.*[20] have shown that longitudinal composite action is much less dependable and is consequently not included herein.

Fig. 4 shows the cross-section of a composite diaphragm. The adjacent deck panels are interconnected with wood splines. The wood splines shown in Fig. 4 have dimensions of 7.7×3×440 cm and are made of Douglas Fir. We can reasonably introduce the idea of effective flange width, as the timber main beams have configurations similar to concrete T-beams, rather than plate girders.

Next, we take the width B, equal to the spacing of the diaphragms, as the effective width of the glulam timber deck. The moment of inertia I_c of a composite diaphragm expressed in terms of steel is given as

$$I_c=I_s+\frac{1}{n}I_w+A_sd_s^2+\frac{1}{n}A_wd_w^2, \quad \cdots\cdots (3)$$

where the subscripts w, s, and c refer to the centroids of the timber deck, steel diaphragm and composite diaphragm, respectively. $A_s=2\times A_1$ is the sum of cross-sectional areas of the chord members, $A_w=B\times T$ is the cross sectional area of the effective timber deck, and $n=E_s/E_{//y}$. $E_{//y}$ is the parallel to grain Young's modulus of the timber deck about the y-axis, as shown in Fig. 4. The distances d_s and d_w from Eq. (3) are shown in Fig. 4 and are given as

$$d_s=\frac{A_wd/n}{A_s+A_w/n}, \quad d_w=d-d_s \quad \cdots\cdots (4\cdot a, b)$$

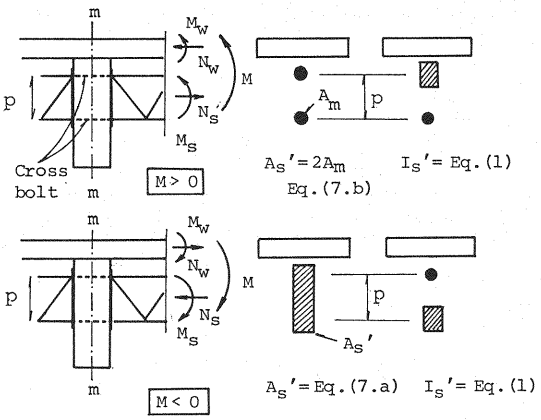

Fig. 5 Modeled cross sections (m-m) of the cross bolts.

Eqs. (3) and (4) are analogous to the formulas for steel-concrete composite girders.

The moment of inertia of the composite cross bolts differs somewhat from that of the composite diaphragm developed above. In Fig. 5, if a positive couple, M_s, is developed in the diaphragm, a tensile force N_s is developed in the cross bolts. Then, the cross-sectional area A_s in Eq. (3) and (4) must be replaced by the sum of cross sectional area of cross bolts, that is, $A_s'=2\times A_m$.

Conversely, if a negative couple develops in the diaphragm, the cross bolts cannot resist the normal compressive force N_s. Thus the elastic timber main beam must resist the force N_s. In the case of negative moment, the cross-sectional area A_s in Eq. (3) and (4) must be replaced by A_s', as shown in Fig. 5. The method for estimating A_s' is illustrated in Fig. 1 (d). Similar to Fig. 1 (c) for bending moment, it is assumed that the reactive normal stress distributes into the timber beam prismatically. The strain energy stored in the timber beam is $N^2b/2E_sA_s'$, i. e. simply the strain energy of a steel bar having a length b.

The moment of inertia I_s' for the cross bolts is the same value both for positive and negative bending moments, as shown in Fig. 5, i. e. I_s' is given by Eq. (1). Collecting the previously developed quantities, we have the following:

$$I_c'=I_s'+\frac{1}{n}I_w+A_s'd_s^2+\frac{1}{n}A_wd_w^2 \quad \cdots\cdots (5)$$

$$d_s=\frac{A_wd/n}{A_s'+A_w/n} \quad \cdots\cdots (6)$$

$$A_s'=\frac{b(v-g)}{n'\cdot\ln\dfrac{v(g+b)}{g(v+b)}} \quad (\text{for } M<0), \quad A_s'=2A_m \quad (\text{for } M>0) \quad \cdots\cdots (7\cdot a, b)$$

3. TIMBER MAIN BEAMS

It has been summarized in Ref. 3) that the optimum load transfer mechanism to provide effective shear and moment transfer between adjacent deck panels for minimizing differential deflections is the use of steel dowels inserted into the edges of the deck panels. In addition, if the attachment of the deck panels to the main beams and of the steel dowels into predrilled lead holes located at the neutral axis of the deck panels are carefully constructed, the mechanical interconnection also preduces a degree of composite action between main beams and deck panels. However, the Akita Cedar species used in the Uyashinai bridge, and generally available in Japan, is a softer wood compared to Douglas Fir, which is most commonly used for timber bridges in the U. S. A. Comparing the Young's moduli of glulam timber beams made of the respective species, (Akita Cedar)/(Douglas Fir) equals 80 000 kg/cm^2/127 000 kg/cm^2=1/1.6 for typical design values. Consequently, it was judged that it is valid to use wood splines rather than steel dowels, as the

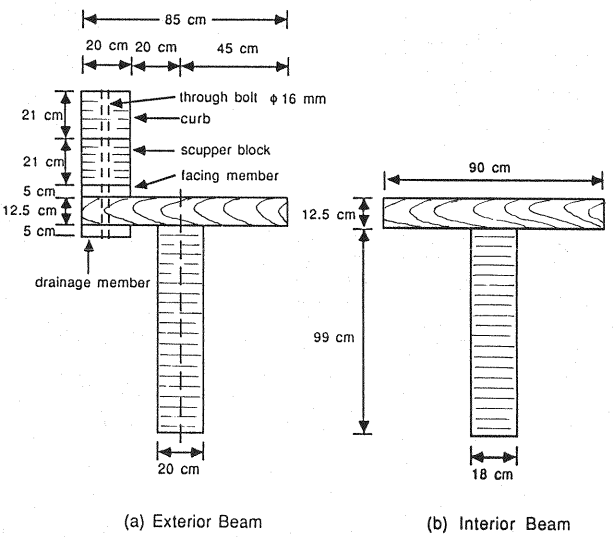

Fig. 6 Exterior and interior beams for moments of inertia.

wood splines can distribute the shear and moment along the edges of the deck panels, if they are suitable constructed.

The deck panels connected with wood splines have some partial structural continuity[21] in the direction of bridge axis as well as in the transverse direction. However, composite action between main beams and deck panels was not observed in the field tests of the Boukawa Bridge[18]. Two reasons were considered for the non-composite action. One was due to unavoidale gaps in adjacent deck panels. The other was due to small Young's modulus of elasticity $E_{\perp y}$ which represents that perpendicular to grain of deck panels (in the direction of y axis in Fig. 4); $E_{\perp y}$ to $E_{\parallel x}$ ratio is $1/n''=E_{\perp y}/E_{\parallel x}=1/27$, as shown in Table 2, where $E_{\parallel x}$ is for main beams (pararel to grain). Herein, we consider that the main beam and the deck are constituting independent beams. Fig. 6 shows the cross-sections of the exterior main beam (with the curb), and the interior main beam. For the exterior beams, it is considered that the curb and deck panels are composite, i. e. that they are essentially one body due to the use of through bolts at suitably arranged scupper blocks. This means that we neglect interlayer slip which would reduce the stiffness. Thus, the moment of inertia of the exterior beam is the sum of composite curb/deck flange and the independent main beam. The moment of inertia of the interior beam is the sum of the values for the deck panel and the main beam without composite action. The calculated values of moment of inertia are given in the next section.

4. RESULTS OF FIELD TESTS[24]

(1) Dimensions and properties

Table 1 shows the cross-sectional properties of the composite diaphragm and cross bolt. The values of Young's moduli, $E_{\parallel x}$ and $E_{\parallel y}$, are based on the Specifications and Commentaries of JSAE[10] at the time of the field tests. Table 2 shows the moments of inertia and torsional constants of the main timber beams, based on the procedure illustrated in the previous section. The torsional constant J_s is for the main beams only and does not include the effect of the deck panels.

The test values of Young's modulus $E_{\parallel x}$ of the five timber main beams are given in Table 3. The tests were done at the glulam timber workshop in Noshiro, Akita Prefecture before the transportation of bridge materials to the field. Fig. 7 shows the non-destructive test procedure for obtaining values of Young's modulus for the actual beams. The span of the timber beams is the same as the actual bridge and the weight of the H-beam used for loading in the bending tests is 232 kg. The Young's modulus is calculated by

Table 1 Section properties of the composite cross beam and cross bolt.

	Properties	Values	
Diaphragms	$n = E_s/E_{\parallel y}$	30	
	$A_s = 2A_1$ (Eq. (3))	11.60 cm^2	
	I_s (Eq. (2))	2,903 cm^4	
	$A_w = B \times T$	4,250 cm^2	
	$I_w = BT^3/12$	55,339 cm^4	
	d_s (Eq. (5.a))	32.64 cm^2	
	d_w (Eq. (5.b))	2.60 cm^2	
	I_c (Eq. (3))	18,064 cm^4	
Cross Bolt	$n' = E_s/E_{\perp x}$	700	
	I'_s (Eq. (1))	504 cm^4	
		$M > 0$	$M < 0$
	A'_s (Eq. (7))	14.14 cm^2	1.42 cm^2
	d_s (Eq. (4) or (6))	32.05 cm	34.90 cm
	d_w (Eq. (4.b))	3.20	0.35 cm
	I'_c (Eq. (5))	18,325 cm^4	4096 cm^4
$E_s = 2.1 \times 10^6$ kg/cm^2, $E_{\parallel y} = 70000$ kg/cm^2 $E_{\parallel x} = 80000$ kg/cm^2, $E_{\perp x} = 3000$ kg/cm^2			

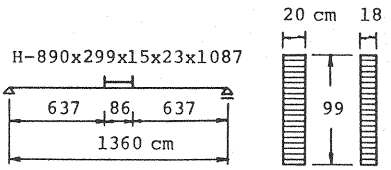

Fig. 7 Span and loading conditions for the bending tests.

Table 2 Moment of inertia and torsional constants of the main beam.

Interior Beam	I	1,455,992 cm^4=$\frac{bh^3}{12} + \frac{BT^3}{12n''}$
	J_s	192,456 cm^4=$\frac{1}{3}b^3h$
Exterior Beam	I	1,927,479 cm^4 composite curb and deck + main beam
	J_s	264,000 cm^4
($n'' = \frac{E_{\parallel x}}{E_{\perp y}}$, where $E_{\perp y} = 3000$ kg/cm^2, $E_{\parallel x} = 800000$ kg/cm^2)		

Table 3 Young's modulus $E_{\parallel x}$.

Girder No.	$E_{\parallel x}$, kg/cm^2 (MPa)
a	90095 (8829)
b	83812 (8214)
c	83736 (8206)
d	81766 (8013)
e	78788 (7721)
Mean	83639 (8197)
Standard Deviation	3708 (363)
Coefficient of Variation	0.044

measuring the deflections at midspan of the timber beams and using the conventional formula of structural engineering. As shwon in Table 3, the mean value of Young's modulus is 83 639 kg/cm^2 (8 197 MPa) and exceeds the normal value of the first class of glulam timber (80 000 kg/cm^2=7 840 MPa) by 4.4 %. The coefficient of variation is no more than 4.4 %.

(2) Grillage stiffness

We have presented a modified grillage stiffness for the grillage timber bridge (see Ref. 17)) before the timber deck panels are attached. The idea of the modified grillage stiffness is now developed for the timber bridge after the attachment of deck panels. Representing the formulas in terms of present symbols, these are as follows:

$$Z=\left(\frac{l}{2a}\right)^3 \cdot \frac{E_s I_c}{E_{\parallel x} I}, \quad Z'=\left(\frac{l}{2a}\right)^3 \cdot \frac{E_s I'_c}{E_{\parallel x} I'}, \quad \cdots\cdots (8\cdot a, b)$$

where Z and Z' are the grillage stiffnesses in bending for the composite diaphragm and for the composite cross bolts, respectively. l and a are the span of the bridge and the on-center spacing of main beams, respectively. As shown in Figs. 1 and 2, the length q of the truss diaphragm nearly equals the on-center spacing a of main beams. The length b of cross bolts does not equal the distance a, but instead equals the width of the main beams. Consequently, the value Z' obtained from Eq. (8·b) underestimates the actual grillage stiffness of the cross bolts. This means that we have conservatively estimated the grillage stiffness of cross bolts.

As can be seen in Table 1, the moments of inertia of composite diaphragm and cross bolts are:

I_c=18 064 cm^4 for the cross beam

I'_c=18 325 cm^4 ($M>0$)
I'_c= 4 096 cm^4 ($M<0$) for the cross bolts

The corresponding non-dimensional grillage stiffnesses become:

$Z=161$ for the cross beam

$Z'=163$ $(M>0)$
$Z'=36$ $(M<0)$ for the cross bolts

Herein, it is interesting to examine grillage stiffness, assuming that no composite action occurs and the stiffness of deck panels can be neglected. In Eq. (8·a, b), replacing I_c to I_s and I'_c to I'_s in Table 1, respectively, we obtain

$Z=26$ for the non-composite cross beam

$Z'=4.4$ for the non-composite cross bolts

It has been noted that if the grillage bridge has the value of grillage stiffness greater than ten, sufficient load distribution can be achieved (see Ref. 19)). If we neglect composite action of deck panels, the value $Z'=4.4$ of the stiffness of cross bolts will be insufficient for load distribution. This has also been pointed out in Ref. 17), 18). Thus, in the present case, it is valid to use the minimum value of $I'_c=4\,096$ cm^4 corresponding to the cross bolts throughout the transverse diaphragm system, for the grillage analysis. One more factor needed is the grillage torsional stiffness. Developing the concept of a grillage torsional stiffness for the timber grillage bridge studied now, in a manner similar to Eq. (8), we can obtain the following:

$$Z_t=\frac{l}{2a}\cdot\frac{E_sI_c}{G_wJ_s},\quad Z'_t=\frac{l}{2a}\cdot\frac{E_sI'_c}{G_wJ_s},\qquad\cdots\cdots(9\cdot a,\ b)$$

where G_w and J_s equal the shearing modulus of wood and the torsional constant of the main timber beam, respectively. The value of G_w equals 4 000 kg/cm^2 (392 MPa) for the glulam timber, from the Specifications and Commentaries of JSAE (see Ref. 10)) and the values of J_s are given in Table 2. The values of Z_t and Z'_t, which correspond to the composite diaphragm and composite cross bolts, respectively, are given for the interior main beams as

$Z_t=93$ for the composite cross beam

$Z'_t=94$ $(M>0)$
$Z'_t=21$ $(M<0)$ for the composite cross bolts

We can, therefore, neglect the effects of torsional rigidity of main beams, for any combination of the values of $(Z, Z_t)=(161, 93)$, $(Z', Z'_t)=(163, 94)$ and $(Z', Z'_t)=(36, 21)$, respectively (see Ref. 19)).

(3) Loading conditions

After paving the wearing surface, the field tests were done by using a truck loaded with concrete blocks and having a total weight of 13.7 tons. In Table 4, the dimensions and the weights on the axles of truck used are shown. The Uyashinai Bridge has one lane as shown in Fig. 2 and, therefore, one truck on the bridge was sufficient to simulate the design loading. Setting the rear axles at midspan of the bridge, the midspan vertical deflections of the main beams and the displacements adjacent to the supports were

Table 4 Dimensions of the truck.

Spacing of truck axles	4.00 m
Load lane width of front axles	1.56 m
Load lane width of rear axles	1.75m
Total weight	13.70 ton (134.3 kN)
Weight on front axles	2.74 ton (26.9 kN)
Weight on rear axles	10.96 ton (107.4 kN)

Photo 1 Loading condition with curbs in place.

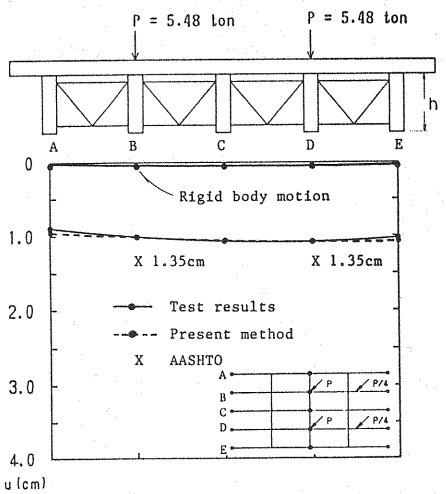

Fig. 8 Deflection diagrams at midspan without the curbs.

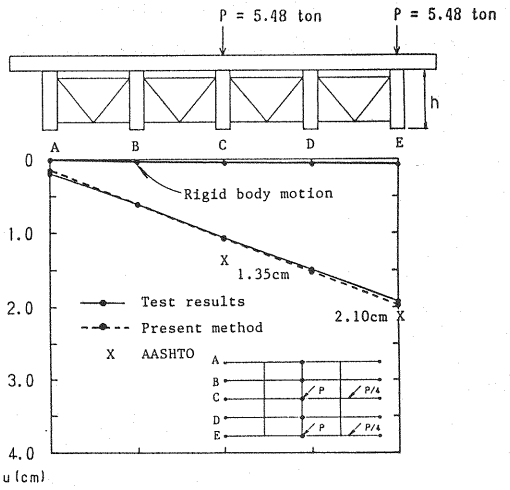

Fig. 9 Deflection diagrams at midspan without the curbs.

measured with dial gauges.

Photo 1 shows a loading condition under testing and the scaffolding set-up for measuring the bridge displacements.

(4) Test results

The test results for deflection of the main beams at midspan of the bridge before the attachment of the curb are shown in Figs. 8 and 9. The solid lines show the test results and the dashed lines show the present grillage beam analysis by the matrix stiffness method. Intersecting points of the main beams and diaphragms are selected as nodal points. Consequently, the number of elements is 31 (20 main beam elements and 12 diaphragm elements). The loading conditions and the rigid body displacements of cross section at midspan are also shown in the figures. The rigid body displacements are the average of the values at the supports and thus, produce the rigid body motions of the main beams at midspan of the bridge. These support motions are due to the elasticity of the neoprene pads. The test results and the results of the present method are corrected by subtracting the rigid body displacements at midspan from the measured absolute deflections.

The deflection diagrams in Fig. 8 reveal somewhat downward convex curvature and those in Fig. 9 are nearly inclined straight lines. As discused in section 3. (2), these show that the composite cross systems of the grillage bridge tested contribute to effective load distribution. In Fig. 9, the rigid body displacement of beam E at midspan due to elastically sinking supports is maximum and is no more than 3.0 % of the measured value for the absolute deflection of beam E. This is similar for the other main beams and also for the main beams in Fig. 8.

Herein, it is interesting to compare the test results with results due to AASHTO. Load distribution factors (D. F.) for glulam panel deck, for single lane glulam beam bridges are

$S/4.5$ for 6 in. deck thickness, and

$S/6.0$ for 4 in. deck thickness

where S=the average beam spacing in feet (see Table 3. 23. 1 in AASHTO). As shown in Fig. 2, S=90 cm $\fallingdotseq$3 feet, and the deck thickness is T=12.5 cm$\fallingdotseq$5 inches for the present bridge. Let us employ the average value for 6 in. and 4 in. deck thicknesses, which gives (for an interior beam) D. F. $=(3/4.5+3/6.0)/2=0.585$. The maximum bending moment, M_{LL}, for a T-14 line loading equals 21 082 kg·m[22]$=154.8$ ft-kips. D. F. for exterior beams A and E (see Figs. 8 and 9) are approximately equal to 1.0, as the centerline of the truck wheels is nearby on the exterior beam. Using a semi-emperical formula[23], the

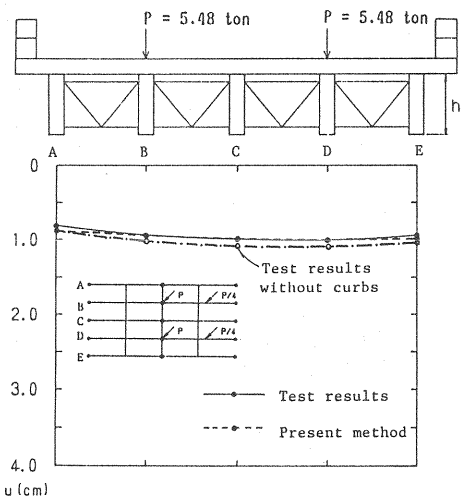

Fig. 10 Deflection diagrams at midspan with the curbs.

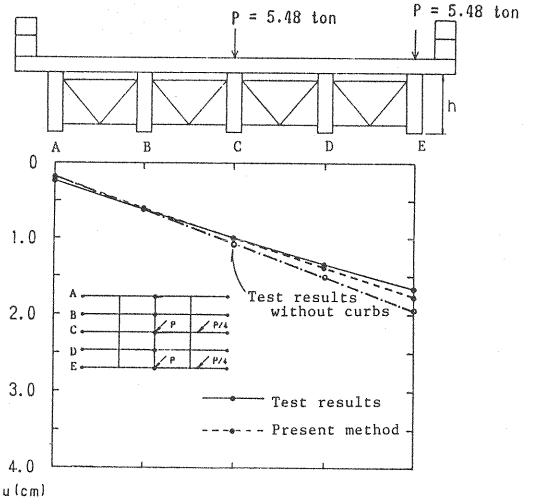

Fig. 11 Deflection diagrams at midspan with the curbs.

maximum deflections of the stringers are

$$\Delta_{LL}=\frac{(\text{D.F.})M_{LL}l^2}{10\,I}=\frac{1\times154.8\times45.3^2}{10\,(20\times99^3/12)/2.54^4}$$

$=0.82$ in. $=2.10$ cm for exterior stringers

$$\Delta_{LL}=\frac{0.585\times154.8\times45.3^2}{10\,(18\times99^3/12)/2.54^4}=1.35\text{ cm}$$

for interior stringers.

where Δ_{LL} corresponds to the deflection u represented with vertical axis in Fig. 8 and 9.

The deflections Δ_{LL} shown in Figs. 8 and 9 (represented by the symbol×) overestimate the test value by 30 % at beam B, which is the maximum overestimation. In Fig. 9, Δ_{LL} only overestimates the test value by 9 % at the exterior beam E. This is surprisingly coincident with the test value, considering the simplicities of the formulae for D. F. and of the semi-empirical methods used.

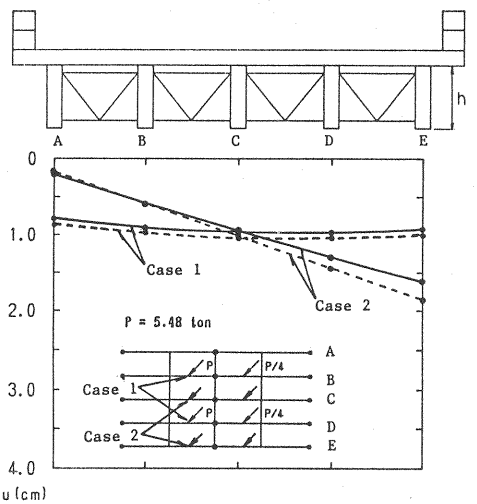

Fig. 12 Deflection diagrams at midspan for other loadings (—— with curbs, ------ without curbs).

Figs. 10 and 11 show the test results together with the present numerical solutions for the loadings after the attachments of the curb. As shown in Fig. 6, and in Table 2, we assumed that the curb, the facing member for the pavement, the drainage member for water cutting, and the partial deck panel have composite action, due to the use of through bolts at suitably arranged scupper blocks. The loading conditions in Figs. 10 and 11 correspond to those in Figs. 8 and 9, respectively.

The solid lines in Figs. 10 and 11 connecting the test values and the dashed lines of the present numerical solutions are very close to each other. The dotted lines in Figs. 10 and 11 show the test results without the curb which are the same as the solid lines in Figs. 8 and 9. In the case of the loading condition of Fig. 10, the effect on deflection of the middle main beam C is about 7.0 % and of Fig. 11, that of exterior main beam E, is about 13 %. In the Boukawa Bridge[18], these values amount to from 40 % to 60 %, as the bridge has a short span of 5.6 m.

Finally, Fig. 12 shows another loading condition in which the rear wheel axles are located at the

midpoints of adjacent steel diaphragms. The loading conditions in the direction of the road width are the same as from Figs. 8 to 11. In Fig. 12, the test results with or without the curb only are shown, as the numerical solutions coincide very closely with the test data. The composite action due to the attachment of the curb is almost of the same degree as the loading conditions of Figs. 10 and 11. Consequently, we have an obvious conclusion that the composite action due to the attachment of curb cannot be neglected to understand well the behavior of timber beam bridges, although in the actual timber bridge design, the composite action can conservatively be neglected.

5. CONCLUSIONS

The Uyashinai Bridge is constructed as a forest roadway bridge which is intended for low traffic volume consisting of heavily-loaded logging trucks. The bridge system employs glulam beams supporting glulam deck panels and an asphaltic wearing surface. This type of timber bridge is the second bridge of its type in Japan, though in U. S. A. it is a commonly used type of bridge. The clear span of 13.6 m (45.3 ft) is the longest in Japan to date for a glulam timber bridge. We obtain the following conclusions, through full scale field tests and numerical solutions.

(1) We can deduce composite action of the deck panels and steel diaphragms, i. e. with respect to the bending of diaphragm systems about the bridge axis, as the experimental deflection diagrams of the cross-section at the midspan of the bridge are closely coincident with the results of numerical analysis performed assuming the composite action.

(2) The concept of the grillage stiffness in bending is conveniently available for the timber grillage bridge and we can predict the circumstances of load distribution, knowing the value of grillage stiffness in bending.

(3) The moment of inertia of composite cross bolts is nearly equal to that of the composite diaphragm, if the cross-sectional area of cross bolt is also nearly equal to that of the chord member of the steel diaphragm and if a positive bending moment acts at the composite cross bolts.

(4) The moment of inertia of composite cross bolts reduces to 1/4.5 times the value of the composite diaphragm if a negative bending moment acts at the composite cross bolts. The grillage stiffness in bending of the composite cross bolts in this case, however, can attain the magnitude of the grillage stiffness being assumed in the bridge design. We can use the moment of inertia of the composite cross bolts for numerical analysis by stiffness matrix methods as the representative value of the stiffness of cross systems, because of the minimum value of stiffness.

(5) The composite action due to the attachment of the curb to the deck panels cannot be neglected if one is to closely predict the behavior of a timber beam bridge. However, in actual timber bridge designs the composite action is not be considered in the codes.

Timber bridges have the most pleasant appearance in the wooded surroundings. However, timber products in Japan today (including glulam timber) are still costly. Annual review of the performance of the Uyashinai Bridge is planned.

6. ACKNOWLEDGEMENTS

The authors wish to acknowledge to K. Hasebe, Assistant Prof. in the Department of Civil Engineering, Akita University, for his numerical checking, drafting etc. and to Steven A. Malers, Graduate Research Assistant in the Department of Civil Engineering, Colorado State University, for his corrective word-processing of manuscript, K. Tsukada in the Akita Office of the Forest Service, Japanese Department of Agriculture and many other Forest Service personnel who also participated in the field tests.

REFERENCES

1) "Specifications for Timber Roadway Bridges", Japanese Ministry of Construction, 1940.
2) Fukuda, T. : Timber Engineering (in Japanese), edited by JSCE, Sobunsya, 1949.
3) Gutkowski, R. M. and Williamson, T. G. : Timber Bridges-Developments and Trends in North America, 11th World Congress of the International Association of Bridge and Structural Engineers, 1980.
4) Gutkowski, R. M. and Williamson, T. G. : Timber Bridges : State-of-the Art, Jour. of Struct. Eng., ASCE, Vol. 109, No. 9, pp. 2175-2191, 1983.
5) Gutkowski, R. M. and Williamson, T. G. : Heavy Timber Structures and Bridges, Structural Wood Research-State of the Art and Research Needs, ASCE, pp. 111-130, 1983.
6) "Specifications for Highway Bridge, American Association of State Highway and Transportation Officials", 13th edition, 1983.
7) Scarisbrick, R. : Laminated Timber Logging Bridges in British Columbia, Jour. of the Struct. Division, ASCE, Vol. 102, No. ST1, pp. 19-34, 1976.
8) Verna, J., Graham, J., Shannon, J. and Sanders, P. : Timber Bridge ; Benefits and Costs, Jour. of the Struct. Engrg., ASCE, Vol. 110, No. 7, pp. 1563-1571, 1984.
9) "Specifications and Commentaries for Roadway Bridge", Japanese Association of Roadway Officials (in Japanese), 1980.
10) "Specifications and Commentaries for Timber Construction", Japanese Society of Architectural Engineering (in Japanese), 1973.
11) McCutcheon, W. J. and Tuomi, R. L. : Procedure for Design of Glued-Laminated Orthotropic Bridge Decks, USDA Forest Service Research Paper FPL 210, 1973.
12) McCutcheon, W. J. and Tuomi, R. L. : Simplified Design Procedure for Glued-Laminated Bridge Deck, USDA Forest Service Research Paper FPL 233, 1974.
13) Tuomi, R. L. and McCutcheon, W. J. : Design Procedure for Glued-Laminated Bridge Decks, USDA Forest Products Jour., Vol. 23, No. 6, 1973.
14) Tuomi, R. L. : Erection Procedure for Glued-Laminated Timber Bridge Decks with Dowel Connectors, USDA Forest Service Research Paper FPL 263, 1976.
15) Gutkowski, R. M. : Glulam Bridge Dowel Systems, Jour. of the Struct. Division, ASCE, Vol. 105, No. ST8, pp. 1712-1716, 1979.
16) Sanders, W. W. : Load Distribution in Glulam Timber Highway Bridges, Final Report to American Institute of Timber Construction, Engineering Research Institute, Iowa State University, 1980.
17) Hasebe, K. and Usuki, S. : A Theoretical Analysis and Experimental Study on a Grillage Girder Using Glued Laminated Timber, Proc. of JSCE, No. 397／VI-9, pp. 85-94, Nov. 1988.
18) Hasebe, K. and Usuki, S. : Analysis and Tests for Composite Action in Glued Laminated Grillage Timber Bridges, Proc. of JSCE, No. 403／VI-10, pp. 269-272, March, 1989.
19) Takasima, H. : Simplified Design Procedure of Load Distributions of Roadway Bridges, the first volume, Gendai-Rikogaku-Publisher (in Japanese), 1985.
20) Gutkowski, R. M., Goodman, R. R. and Pault, J. D. : Tests and Analysis for Composite Action in Glulam Bridges, Transportation Research Record 676, National Academy of Sciences, 1978.
21) Usuki, S., Ishida, S. and Kamei, Y. : Analysis and Experiments on Orthotropic, Continuous Deck Panels, Engineering Reports of Tohoku Prefecture, JSCE, pp. 8-9 (in Japanese), 1988.
22) Usuki, S. : Design and Construction Methods of Glulam Timber Beam Bridge, Dobokuseko, Vol. 30, No. 10, pp. 87-92 (in Japanese), Oct. 1989.
23) Gutkowski, R. M. : Short Course Notes, Engineered Timber Structures, Dept. of Civil Engineering, Colorado State University, Sept., 1988.
24) Hasebe, K. and Usuki, S. : Field Tests and Analysis of Uyashinai Forest Road Bridge Using Glued Laminated Timbers, Jour. of Structural Engrg., Vol. 35 A, pp. 879-887, 1989.

(Received January 19 1990)